A *PRIMPOL* mutation and variants in multiple genes may contribute to phenotypes in a familial case with chronic progressive external ophthalmoplegia symptoms

Kei Kasamo, Masayuki Nakamura, Yoko Daimou, Akira Sano

Kagoshima University Graduate School of Medical and Dental Sciences, Department of Psychiatry, Kagoshima, Japan

8-35-1 Sakuragaoka, Kagoshima 890-8520, Japan.
Phone: +81-99-2755346

***Corresponding author:**
Masayuki Nakamura
8-35-1 Sakuragaoka, Kagoshima 890-8520, Japan.
Phone: +81-99-2755346
nakamu36@m.kufm.kagoshima-u.ac.jp

Total number of page: 22

Total number of figure: 1

Total number of tables: 2

Total number of supplementary Table: 1

Abstract

Chronic progressive external ophthalmoplegia (CPEO) is one of the most common mitochondrial disorders. It is characterized by bilateral, slowly progressing loss of extraocular muscle mobility, orbicularis oculi weakness, ptosis and other neuromuscular symptoms, which are caused by the accumulation of multiple mitochondrial DNA (mtDNA) deletions. Many mutations in different nuclear genes, such as *POLG1*, *POLG2*, *ANT1,* and others, have been described as causing autosomal-inherited CPEO with multiple mtDNA deletions. Most causative genes are involved in mtDNA replication impairment. Here, we report a family with CPEO-like symptoms characterized by multiple muscle mtDNA deletions, ptosis, diabetes, hearing loss, mental retardation, and emotional instability. We performed genetic analyses to identify nuclear gene mutations in the family. DNA from the proband was analyzed by whole-exome sequencing. In addition to possible pathogenic mutations, rare variants were prioritized for gene-functional phenotype interpretation. We found possible pathogenetic mutations in the *PRIMPOL*, *BRCA1*, *CPT2*, and *GJB2* genes, and functional polymorphisms in the *CARD8,* and *MEFV* genes. Multiple functional polymorphism and possible pathogenic mutations may contribute to mitochondrial-disease-like phenotypes in a composite manner.

Abbreviations

mtDNA, mitochondrial DNA; CPEO, chronic progressive external ophthalmoplegia; PCR, polymerase chain reaction; SNPs, single nucleotide polymorphisms; MAF, minor allele frequency; CPTII, carnitine palmitoyltransferase II; FMF, familial Mediterranean fever; PFAPA, periodic fever, aphthous stomatitis, pharyngitis and cervical adenitis;

CARD8, caspase recruitment domain containing protein 8; NLRPs, nucleotide-binding oligomerization domain leucine-rich repeat, and the pyrin domain containing proteins

Keywords:

Progressive external ophthalmoplegia, Multiple mitochondrial DNA deletions, Whole-exome sequencing, *PRIMPOL*

1. Introduction

Mitochondrial diseases can be caused by multiple mitochondrial DNA (mtDNA) deletions, point mutations, or depletion, as a result of mutations in either mtDNA itself or nuclear genes. Chronic progressive external ophthalmoplegia (CPEO) is one of the most common mitochondrial disorders, and is characterized by bilateral, slowly progressive loss of extraocular muscle mobility, orbicularis oculi weakness, and ptosis (Biousse and Newman, 2001). Additional commonly observed features are weakness in other muscles, short stature, diabetes mellitus, deafness, cardiac conduction defects, central and peripheral respiratory dysfunction, endocrine and sex organ abnormalities, and various neuropsychiatric symptoms (Kato et al., 2011).

CPEO is typically associated with multiple deletions in muscle mtDNA and ragged red fiber in muscle pathology (Zeviani et al., 1989). Inheritance is reported to be autosomal dominant (Zeviani et al., 1989), recessive (Bohlega et al, 1996), or digenic (Van Goethem et al., 2003), and nuclear gene mutations have been reported to cause multiple mtDNA deletions and to result in CPEO. These include mutations in *POLG* (Van Goethem et al., 2001), *POLG2* (Longley et al., 2006), *C10orf2* (Spelbrink et al., 2001), *SLC25A4* (Kaukonen et al., 2000), *ECGF1* (Nishino et al., 1999), *OPA1* (Alexander et al., 2000 ; Delettre et al., 2000), *WFS1* (Inoue et al., 1998), and *RRM2B* (Tyynismaa et al., 2009 ; Takata et al., 2011).

In this study, we performed a mutation analysis, involving whole-exome sequencing of a family with CPEO symptoms. The analysis revealed that complex relationships may exist between the identity of family members and multiple mutations in the *PRIMPOL*, *BRCA1*, *CPT2*, and *GJB2* genes, functional polymorphisms in the *CARD8,* and *MEFV*

genes. *PRIMPOL* encodes PrimPol protein, which has both DNA dependent RNA/DNA primase and DNA polymerase activities. A mutation in *PRIMPOL* may be a novel candidate for causing mtDNA multiple deletions in human mitochondrial disease.

2. Subjects and methods

2.1. Case report

The proband (Fig. 1) was a 69-year-old male whose parents were suspected to have been consanguineous, and who was born with a low birth weight (2000 g) and congenital deafness. The proband presented with developmental delay and mental retardation. By the age of 20, the proband had been diagnosed with diabetes mellitus, and in his thirties was admitted to a psychiatric hospital for one month due to psychotic behavior. In his sixties, the proband developed cognitive decline, bilateral ptosis, external ophthalmoplegia, cataracts, muscle weakness, and emotional instability. At the age of 69, the proband was admitted to our hospital with suspected CPEO, where he presented with short stature (141 cm) and low body weight (34 kg), with a body mass index of 17.1 and severe bilateral sensorineural hearing loss (both sides 105 dB). The ophthalmological evaluation showed, visual acuity was 0.3 in right, and 0.2 in left. We observed elevated CSF lactate (22.0 [4.2–17.0] mg/dl) and pyruvate (1.2 [0.3–0.9] mg/dl) concentrations, along with bilateral oculomotor disturbance, dysphagia, and decreased deep tendon reflexes. An echocardiogram revealed mild left ventricular hypertrophy and mild aortic valvular stenosis. Electroencephalography revealed a slow-wave abnormality, and nerve conduction studies showed specific motor and sensory neuropathy. Brain MRI revealed general cerebral atrophy and symmetrical T2 and FLAIR high-intensity, along with T1 low-intensity periventricular regions and spots in

the deep white matter, basal ganglia, and thalamus (Fig. 1). Muscle histopathology revealed a moderately variable fiber size but no ragged red fiber or COX-deficient fiber. Following discharge, the proband died of aspiration pneumonia at the age of 71.

2.2. Familial history

The pedigree of the proband is shown in Figure A. II–2 was his 80-year-old second-eldest sister, who was 135 cm tall and weighed 42 kg. She presented with diabetes, hearing loss, mental retardation, and gradually progressive cognitive dysfunction. Brain CT imaging revealed low periventricular density. III–10 had a history of hypothyroidism and diabetes and died suddenly of suspected aortic dissection. II–3 and IV–1 showed no symptoms. Their visual acuities were unknown.

2.3. Genetic analysis

Written informed consent was obtained from the proband, II-2, II-3, II-5, III-10, and IV-1 at the time of blood sampling (Fig. 1). The research protocol and consent form were approved by the Institutional Review Boards of Kagoshima University.

2.4. Sequence analysis of mtDNA

The entire mtDNA sequence was amplified after designing 27 overlapping polymerase chain reaction (PCR) fragments and identified the sequences of the entire mtDNA of the proband's leukocyte. Reactions were performed as described by Kato et al (Kato et al., 2011). All PCR fragments were sequenced and the variants were

compared with the Mitomap database (http://www.mitomap.org/), GenBank and PubMed/MEDLINE-listed publications.

2.5. PCR-Southern blot analysis of mtDNA

Polymerase chain reaction (PCR)-Southern blot analyses were performed to detect large deletions of mtDNA from the muscle of the proband and leukocytes of the proband and II-2, II-3, II-5, III-10. PCR reactions were performed using *TaKaRa LA Taq* with GC Buffer (Takara, Kyoto, Japan). Reactions were performed in a total volume of 25 μl containing 20 ng of each DNA sample, 0.2 μM each of the forward and reverse oligonucleotide primers (Kato et al., 2011), 12.5 μl 2 × GC Buffer I containing 2 mM of $MgCl_2$ (TaKaRa), 0.2 mM each of dATP, dGTP, dTTP and dCTP, and 1.25 units of *TaKaRa LA Taq*. The PCR program was as follows: 94°C for 1 min, 30 cycles of 98°C for 10 s and 64°C for 15 min, followed by 72°C or 10 min. PCR products were separated on 0.8% agarose gels at 100 V for 30 min, then DNA was transferred to a nylon transfer membrane (Hybond-N+, GE Healthcare, Chicago, IL, USA) using the methods of Southern et al (Southern, 1975). An mtDNA probe was synthesized against full-length mtDNA (nucleotide positions 3019–2910). The full-length mtDNA was generated and cloned by PCR using DNA extracted from normal human leukocytes and separated on 0.8% agarose gels. Amplified products were purified using a QIAEX II Gel Extraction kit (Qiagen, Hilden, Germany). The probes were labeled and hybridized using the Gene Images AlkPhos Direct Labeling and Detection system and visualized with CDP-*Star* Chemiluminescent Substrate (GE Healthcare). Images were recorded by a digital analyzer (Fujifilm LAS-1000; Fujifilm, Tokyo, Japan).

2.6. Sequence analysis of nuclear genes

The Sanger sequencing analysis was performed as described by Kato et al (Kato et al., 2011). The coding exons and exon–intron boundaries containing the upstream 1-kb region of the nuclear genes (*POLG*, *POLG2*, *C10orf2*, *SLC25A4*, *ECGF1*, *OPA1*, *WFS1*, and *RRM2B*) were amplified using PCR on genomic DNA that had been isolated from the family members. All PCR products were subjected to Sanger sequencing. PCR reactions were performed in a total volume of 12.5 μl containing 10–30 ng of each DNA sample, 0.2 μM each of the forward and reverse oligonucleotide primers (Kato et al., 2011, Supplementary Table), 0.2 mM each of dATP, dGTP, dTTP, and dCTP, and 0.5 units of TaKaRa Taq. The PCR program was as follows: 94◦C for 2 min, 35 cycles of 94◦C for 30s, 58–64◦C for 30 s and 72◦C for 1 min, followed by 72◦C for 5 min. The amplified PCR products were separated on 1% agarose gels at 100 V for 30 min, and were labeled using a BigDye Terminator v3.1 Cycle Sequencing Kit (Applied Biosystems, Foster City, CA, USA) with the same primers used in the initial PCR and following the protocol described above. Products were then directly sequenced on an ABI PRISM 3130 Avant Genetic Analyzer (Applied Biosystems).

2.7. Whole-exome sequencing

Whole-exome sequencing was performed on the leukocyte of the proband according to the manufacturers' protocol. Genomic DNA was captured with the SureSelectXT Human All Exon v.4 Kit (Agilent Technologies, Santa Clara, CA, USA) and sequenced per lane on an Illumina HiSeq 2000 (Illumina, San Diego, CA, USA) with 101-bp paired-end reads. Image analysis and base calling were performed with sequencing control software using real-time analysis and CASAVA ver.1.8.1 software (Illumina).

Sequencing reads were mapped on the human reference genome GRCh37/hg19 using SeqNova Cloud Server (DNAnexus). The detected variants were confirmed using the traditional Sanger method on an ABI PRISM 3130 Avant Genetic Analyzer (Applied Biosystems). Subsequently, the nuclear genes that were identified by filtering the whole exome sequencing, were analyzed by the Sanger sequencing analysis. The regions containing the variants amplified using PCR on genomic DNA that had been isolated from the family members. Segregation analysis was performed with the detected variants using the traditional Sanger method. (Supplementary Table).

3. Results

3.1. Sequence analysis of mtDNA

No pathogenic mutations were identified in the mtDNA of the proband.

3.2. PCR-southern blot analysis of mtDNA

We performed a PCR-southern blot analysis to detect large deletions of mtDNA with hybridizing probes generated by full-length mtDNA. We found multiple mtDNA deletions in the skeletal muscles but not the leukocytes of the proband (Fig. 1).

3.3. Sanger sequencing analysis of nuclear genes

We performed Sanger sequencing of the nuclear genes associated with multiple mtDNA deletions: *POLG*, *POLG2*, *C10orf2*, *SLC25A4*, *ECGF1*, *OPA1*, *WFS1*, and *RRM2B*. However, we did not identify any pathogenic mutations in the region coding exons or in

exon–intron boundaries containing the region spanning approximately 1 kb upstream of the 5 prime end.

3.4. Whole-exome sequencing

Table 1 summarizes the filtering method used to narrow down candidates. A total of 6.3 Gb of sequence was generated using the Illumina HiSeq 2000 (Illumina). A total of 123,712 variants, including 20,132 single nucleotide polymorphisms (SNPs) and 408 indels, were detected in the coding regions. To identify the mutations associated with mtDNA modification, we performed a keyword search using the human gene database GeneCards (http://www.genecards.org). Ninety-one variants were detected in the genes identified by GeneCards using the search terms “mtDNA” or “replication”. After removing variants with less than 10× coverage, 80 variants remained. To identify possible pathogenic mutations, we picked up four very rare variants in *PRIMPOL*, *CPT2, BRCA1 and APOE* (their minor allele frequency (MAF) ≤ 0.1%). MAF was calculated by the Japanese reference panel project of the Tohoku Medical Megabank (2KJPN). After filtering and segregation analysis, we found three possible pathogenic variants: p.Y89D, p.G275D, and p.V605L, in *PRIMPOL*, *BRCA1*, and *CPT2*, respectively, each of which was heterozygously cosegregated with the phenotypes from II–2 and the proband (Table 2, Fig. 1). We also focused on homozygous variants. After removing variants with less than 10× coverage, 4280 homozygous variants remained. Of these, we selected 29 very rare variants (MAF ≤ 0.1%). Eight variants that were indicated as “benign” by PolyPhen-2 (http://genetics.bwh.harvard.edu/pph2/) were removed. The subsequent Sanger sequencing analysis confirmed a homozygous

frameshift mutation, c.235delC (p.L79Cfs), in *GJB2*, which cosegregated with the hearing-loss phenotype in the studied family. We also found thermolabile polymorphisms, p.F352C and V386I, in *CPT2* in targeted Sanger sequencing for *CPT2* gene. Subsequently, in association with *CARD8*, we found high-fever-associated variants: c.289_290insAA (p.V98Kfs; rs140826611), p.L110P (rs11466018), and p.E148Q (rs3743930) in *CARD8* and *MEFV*, respectively (Table 2, Figure 1).

4. Discussion

In the present study, we sequenced the whole DNA exome from a proband with CPEO symptoms and detected possible pathogenic and/or functional rare variants in *PRIMPOL*, *BRCA1*, *CPT2*, *GJB2*, and functional polymorphisms in *CARD8* and *MEFV*. *PRIMPOL* encodes the PrimPol protein, which is involved in both DNA-dependent RNA/DNA primase and DNA polymerase activity (Bianchi et al., 2013). It has been reported that PrimPol is involved in DNA damage tolerance and translesion synthesis during nuclear replication in eukaryotic cells (Rudd et al., 2014). PrimPol is localized in both the nucleus and mitochondrial DNA (García-Gómez et.al, 2013). The rare p.Y89D mutation promotes cell-viability decline following UV damage *in vitro* and more strongly reduces DNA-replication fork rates compared with PrimPol-knockout cells (Zhao et al., 2013 ; Keen et al., 2014). These results strongly suggest that human cells with the p.Y89D variant have gain-of-functionally impaired mtDNA replication, which may have increased the risk of the multiple muscle mtDNA deletions observed in the proband in this study. Keen et al reported that p.Y89D was associated with high

myopia. On the other hand, Li and Zhang reported that p.Y89D was unlikely to have roles in high myopia because people without ocular disease including high myopia also carried p.Y89D mutation (Li and Zhang, 2015). However, both reports undescribed at all the neuropsychiatric symptoms of those who carried p.Y89D.

Somatic mutations including the rare mutation of p.G275D in the *BRCA1* gene are known to confer a high risk of breast cancer (Zhang et al., 2012). One involvement of BRCA1 protein in addressing DNA damage is in the repair of DNA double-strand breaks through homologous recombination, nucleoside-excision repair, and possibly the non-homologous end-joining pathways (Zhang, 2013). Although to our knowledge no study has reported on the mtDNA repair function of BRCA1 protein, it may play a role in mtDNA repair because it is also localized in mitochondria (Coene et. al., 2005).

Mutations of genes related to mitochondrial metabolism are also heavily involved in mitochondrial dysfunction. *CPT2* encodes carnitine palmitoyltransferase II (CPTII), which is an enzyme localized in the inner mitochondrial membrane and plays a role in mitochondrial β-oxidation by fatty acid accumulation (Bonnefont et al., 2004). The rare p.V605L mutation and the p.F352C and p.V368I polymorphisms are associated with thermal instability in CPTII (Kubota et al., 2012). CPTII encoded by the allele including these thermolabile variants shows moderate enzyme activity at normal body temperature but severely impaired activity in the presence of high fever, resulting in influenza-related encephalopathy (Yao at al., 2008). It has been reported that the dominant-negative effect of *CPT2* mutation could lead to severe activity impairment at high temperatures (Thuillier et al., 2003). Japanese patients with severe influenza-associated encephalopathy carry the three-compound variants p.F352C, p.V368I, and p.V605L in CPTII (Kubota et al., 2012). *In vitro* studies have revealed that cells

transfected with constructions of these variants show significant thermal instability (Yao at al., 2008). In addition, the proband in this study carried homozygous p.V98Kfs in *CARD8* and p.L110P-p.E148Q in *MEFV*. The former mutation may be associated with periodic fever in aphthous stomatitis, pharyngitis, and cervical adenitis syndrome (Cheung et al., 2017), and the latter variants with familial Mediterranean fever (FMF) (Kiyoshi et al., 2016), each of which can decrease CPTII activity through high fever. Functional polymorphisms associated with periodic fever syndrome such as FMF and periodic fever, aphthous stomatitis, pharyngitis and cervical adenitis (PFAPA) syndrome seemed to contribute to a decrease in CPTII activity via high fever. FMF is an autosomal recessive disorder caused by genetic mutations in *MEFV*, which encodes pyrin, a protein that suppresses the function of inflammasome (Bernot et al., 1998). It is characterized by recurring attacks of fever and peritonitis, pleuritis, arthritis, and erysipelas-like skin erythema (Samuels et al., 1998).

CARD8 encodes a caspase recruitment domain containing protein 8 (CARD8), which is also involved in the inflammatory pathway. It interacts with the nucleotide-binding oligomerization domain, leucine-rich repeat, and the pyrin domain containing proteins (NLRPs) which assemble into inflammasome complexes (Ito et al., 2014). The *CARD8* frameshift variant, p.V98Kfs, introduces a premature stop codon, leading to decreased *CARD8* expression, which in turn leads to increased inflammasome activity and IL-1β production (Cheung et al., 2017). Moreover, the functional polymorphisms, p.L110P and p.E148Q, in *MEFV*, which is associated with FMF, were observed in the proband and II-3.

The *GJB2* gene encodes the gap junction protein connexin 26. *GJB2* mutations cause gap junction loss or malfunction, which may disrupt potassium movement from the hair

cells through the supporting cell network back to the endolymphis. These mutations account for up to 50% of congenital deafness (Estivill et al., 1998). In Japanese patients with hereditary hearing loss, the homozygous c.235delC mutation is most commonly found (Abe et al., 2000). The connexin cycle is expected to be especially sensitive to the energy state, and mitochondrial mutations may disrupt cochlear cells from maintaining needed levels of gap junctions (Abe et al., 2001). A synergism may thus exist between c.235delC and mtDNA mutations that reduces the quantity of ATP (Estivill et al., 1998). This suggests that multiple mtDNA deletions found in the proband in this study may have affected the severity of his hearing loss.

The combined results indicate that the mitochondrial-disease-like symptoms observed in the proband can be explained as follows. 1) Polymorphisms in *CARD8* and/or *MEFV* may induce frequent high fever. 2) In response to high fever, thermolabile variants in *CPT2* cause CPTII deficiency, leading to mtDNA damage. 3) With respect to predicted gene function, the *PRIMPOL* mutation is largely responsible for the remaining mtDNA damage, leading to multiple mtDNA deletions, although *BRCA1* mutation may also be involved. These conclusions are supported by the fact that II–2, who carried all the variants and/or polymorphisms except for in *MEFV*, exhibited similar symptoms to the proband. However, II-2 showed no evidence of ptosis. This is probably because she did not carry both p.L110P and p.E148Q in *MEFV*.

Although further studies are needed to functionally validate each genetic defect we identified and to confirm our results and hypotheses, we suggest that multiple variants of mtDNA- or DNA-replication-related genes could potentially combine to cause the complex familial mitochondrial-disease-like symptoms observed in this study. In

particular, *PRIMPOL* mutations may contribute to multiple mtDNA deletions in patients with CPEO via a number of mutation-related pathogenic pathways.

Acknowledgments

The authors thank all involved patients and their families for their participation. The authors also thank Ms. Hiwatashi and Ms. Yokoyama for their technical assistance.

Conflict of Interest

This research did not receive any specific grant from funding agenecies in the public, commercial, or not-for-profit sectors.

References

Abe et al., 2000 S. Abe, S. Usami, H. Shinkawa, PM. Kelley, WJ. Kimberling. Prevalent connexin 26 gene (GJB2) mutations in Japanese. J Med Genet 37 (2000) pp. 41–43.

Abe et al., 2001 S. Abe, PM. Kelley, WJ. Kimberling, S. Usami. Connexin 26 gene (*GJB2*) mutation modulates the severity of hearing loss associated with the 1555A-->G mitochondrial mutation. Am J Med Genet 103 (2001) pp. 334–338.

Alexander et al., 2000 C. Alexander, M. Votruba, UE. Pesch, DL. Thiselton, S. Mayer, A. Moore, M. Rodeiguez, U. Kellner, B.Leo-Kottler, G. Auburger, SS. Bhattacharya, B. Wissinger. *OPA1,* encoding a dynamin-related GTPase, is mutated in autosomal dominant optic atrophy linked to chromosome 3q28. Nat Genet 26 (2000) pp. 211–215.

Bernot et al., 1998 A. Bernot, C. da Silva, J-L. Petit J-L, C.Cruaud, C. Caloustian, V. Castet, M. Ahmed-Arab, C. Dross, M. Dupont, D. Cattan, N. Smaoui, C. Dode, C. Pecheux, B. Nedelec, J. Medaxian, M. Rozenbaum, I. Rosner, M. Delpech, G. Grateau, J. Demaille, J. Weissenbach, I. Touitou. Non-founder mutations in the MEFV gene establish this gene as the cause of familial Mediterranean fever (FMF). Hum Mol Genet 7 (1998) pp. 1317–1325.

Bianchi et al., 2013 J. Bianchi, SG. Rudd, SK. Jozwiakowski, LJ. Bailey, V. Soura, E. Taylor, I. Stevanovic, AJ. Green, TH. Stracker, HD. Lindsay, AJ. Doherty. PrimPol bypasses UV photoproducts during eukaryotic chromosomal DNA replication. Mol

Cell 52 (2013) pp. 566–573.

Biousse and Newman, 2001 Biousse V and Newman NJ. Neuro-ophthalmology of mitochondrial diseases., Semin Neurol 21 (2001), pp. 275–291.

Bohlega et al, 1996 S. Bohlega, K. Tanji, F.M. Santorelli, M. Hirano, A. al-Jishi, S. DiMauro. Multiple mitochondrial DNA deletions associated with autosomal recessive ophthalmoplegia and severe cardiomyopathy. Neurology 46 (1996) pp. 1329–1334.

Bonnefont et al., 2004 J-P Bonnefont, F. Djouadi, C. Prip-Buus, S. G, A. M, J. B. Carnitine palmitoyltransferases 1 and 2: biochemical, molecular and medical aspects. Mol Aspects Med 25 (2004) pp. 495–520.

Cheung et al., 2017 MS. Cheung, K. Theodoropoulou, J. Lugrin, F. Martinon, N. Busso, M. Hofer. Periodic Fever with Aphthous Stomatitis, Pharyngitis, and Cervical Adenitis Syndrome Is Associated with a CARD8 Variant Unable To Bind the NLRP3 Inflammasome. J Immunol 198 (2017) pp. 2063–2069.

Coene et. al., 2005 ED. Coene, MS. Hollinshead, AAT. Waeytens, VRJ. Schelfhout, WP. Eechaute, MK. Shaw, PMV. Van Oostveldt, DJ. Vaux. Phosphorylated BRCA1 is predominantly located in the nucleus and mitochondria. Mol Biol Cell 16 (2005) pp. 997–1010.

Delettre et al., 2000 C. Delettre, G. Lenaers, J-M. Griffoin, N. Gigarel, C. Lorenzo, P. Belenguer, L. Pelloquin, J. Grosgeorge, C. Turc-Carel, E. Perret, C. Astarie-Dequeker, L. Lasquellec, B. Aenaud, B. Ducommun, J. Kaplan, CP. Hamel. Nuclear gene *OPA1*, encoding a mitochondrial dynamin-related protein, is mutated in dominant optic atrophy. Nat Genet 26 (2000) pp. 207–210.

Estivill et al., 1998 X. Estivill, P. Fortina, S. Surrey, R. Rabionet, S. Melchionda, L. D'Agruma, E. Mansfield, E. Rappaport, N. Govea, M. Milla, L. Zelante, P. Gasparini. Connexin-26 mutations in sporadic and inherited sensorineural deafness. Lancet 351 (1998) pp. 394–398.

García-Gómez et.al, 2013 S. García-Gómez, A. Reyes, MI. Martínez-Jiménez, ES. Chocron, S. Mouron, G. Terrados, C. Powell, E. Salido, J. Mendez, IJ. Holt, L. Blanco. PrimPol, an Archaic Primase/Polymerase Operating in Human Cells. Mol Cell 52 (2013) pp. 541–553.

Inoue et al., 1998 H. Inoue, Y. Tanizawa, J. Wasson, P. Behn, K. Kalidas, E. Bernal-Mizrachi, M. Muecker, H. Marshall, H. Donis-Keller, P. Crock, D. Rogers, M. Mikuni, H. Kumashiro, K. Higashi, G. Sobue, Y. Oka, M.Alan Permutt. A gene encoding a transmembrane protein is mutated in patients with diabetes mellitus and optic atrophy (Wolfram syndrome). Nat Genet 20 (1998) pp. 143–148.

Ito et al., 2014 S. Ito, Y. Hara, T. Kubota. CARD8 is a negative regulator for NLRP3 inflammasome, but mutant NLRP3 in cryopyrin-associated periodic syndromes escapes the restriction. Arthritis Res Ther 16: R52 (2014).

Kato et al., 2011 M. Kato, M. Nakamura, M. Ichiba, A. Tomiyasu, H. Shimo, I. Higuchi, S. Ueno, A. Sano. Mitochondrial DNA deletion mutations in patients with neuropsychiatric symptoms., Neurosci Res 69 (2011), pp. 331–336.

Kaukonen et al., 2000 J. Kaukonen, JK. Juselius, V. Tiranti, A. Kyttala, M. Zeviani, GP. Comi, S. Keranen, L. Peltonen, A. Suomalainen. Role of adenine nucleotide translocator 1 in mtDNA maintenance. Science 289 (2000) pp. 782–785.

Keen et al., 2014 BA. Keen, LJ. Bailey, SK. Jozwiakowski, AJ. Doherty. Human PrimPol mutation associated with high myopia has a DNA replication defect. Nucleic Acids Res 42 (2014) pp. 12102–12111.

Kiyoshi et al., 2016 M. Kiyoshi, I. Yasumori, J. Yuka, N. Iwanaga, C. Kawahara, K. Agematsu, A. Yachie, J. Masumoto, K. Fujikawa, S. Yamasaki, T. Nakamura, Y. aubara, T. Koga, Y. Nakashima, T. Shimizu, M. Umeda, F. Nonaka, M. Yasunami, K. Eguchi, K. Yushiura, A. Kawakami. Familial Mediterranean fever is no longer a rare disease in Japan. Arthritis Res Ther 18: 175 (2016)

Kubota et al., 2012 M. Kubota, J. Chida, H. Hoshino, H. Ozawa, A. Koide, H. Kashii, A. Koyama, Y. Mizunom, A. Hoshino, M. Yamaguchi, D. Yao, M. Yao, H. Kido. Thermolabile CPT II variants and low blood ATP levels are closely related to severity of acute encephalopathy in Japanese children. Brain Dev 34 (2012) pp. 20–27.

Li and Zhang, 2015 J. Li, Q. Zhang. *PRIMPOL* Mutaion : Functional Study Does Not Always Reveal the Truth. Investigative Ophthalmology & Visual Science 56 (2015) pp. 1181-1182.

Longley et al., 2006 MJ. Longley, S. Clark, C. Yu Wai Man, G. Hudson, SE. Durham, RW. Taylor, S. Nifhtingale, DM. Turnbull, WC. Copeland, PF. Chinnery. Mutant *POLG2* disrupts DNA polymerase gamma subunits and causes progressive external ophthalmoplegia. Am J Hum Genet 78 (2006) pp. 1026–1034.

Nishino et al., 1999 I. Nishino, A. Spinazzola, M. Hirano. Thymidine phosphorylase gene mutations in *MNGIE*, a human mitochondrial disorder. Science 283 (1999) pp. 689–692.

Rudd et al., 2014 SG. Rudd, J. Bianchi, AJ. Doherty. PrimPol-A new polymerase on the block. Mol Cell Oncol (2014) doi:10.4161/23723548.2014.960754.

Samuels et al., 1998 J. Samuels, I. Aksentijevich, Y. Torosyan, M. Centola, Z. Deng, R. Sood, DL. Kastner. Familial Mediterranean fever at the millennium. Clinical spectrum, ancient mutations, and a survey of 100 American referrals to the National Institutes of Health. Medicine 77 (1998) pp. 268–297.

Southern, 1975 E.M. Southern. J. Mol. Biol 98 (1975) pp. 503-517.

Spelbrink et al., 2001 JN. Spelbrink, F-Y. Li, V. Tiranti, K. Nikali, Q-P. Yuan, M. Tariq, S. Wanrooij, N. Garrido, G. Comi, L. Morandi, L. Santoro, A. Toscano, G-M. Fabrizi, H. Somer, R. Croxen, D. Beeson, J. Poulton, A. Suomalainen, HT. Jacobs, M. Zeviani, C. Larsson. Human mitochondrial DNA deletions associated with mutations in the gene encoding Twinkle, a phage T7 gene 4-like protein localized in mitochondria. Nat Genet 28 (2001) pp. 223–231.

Takata et al., 2011 A. Takata, M. Kato, M. Nakamura, T. Yoshikawa, S. Kanba, A. Sano, T. Kato. Exome sequencing identifies a novel missense variant in *RRM2B* associated with autosomal recessive progressive external ophthalmoplegia. Genome Biol 12: R92 (2011).

Thuillier et al., 2003 L. Thuillier, H. Rostane, V. Droin, F. Demaugre, M. Brivet, N. Kadhom, C. Prip-Buus, S. Gobin, J-M. Saudubray, J-P. Bonnefont. Correlation between genotype, metabolic data, and clinical presentation in carnitine palmitoyltransferase 2 (CPT2) deficiency. Hum Mutat 21 (2003) pp.493–501.

Tyynismaa et al., 2009 H. Tyynismaa, E. Ylikallio, M. Patel, MJ. Molnar, RG. Haller,

A. Suomalainen. A Heterozygous truncating mutation in *RRM2B* causes autosomal-dominant progressive external ophthalmoplegia with multiple mtDNA deletions. Am J Hum Genet 85 (2009) pp. 290–295.

Van Goethem et al., 2001 G. Van Goethem, B. Dermaut, A. Löfgren, J. Martin, C. Van Boeckhoven. Mutation of *POLG* is associated with progressive external ophthalmoplegia characterized by mtDNA deletions. Nat Genet 28 (2001) pp. 211–212.

Van Goethem et al., 2003 G. Van Goethem, A. Löfgren, B. Dermaut, C. Ceuterick, J. Martin, C. Van Broeckhoven. Digenic progressive external ophthalmoplegia in a sporadic patient: recessive mutations in *POLG* and *C10orf2/Twinkle*. Hum Mutat 22 (2003) pp. 175–176.

Yao at al., 2008 D. Yao D, H. Mizuguchi, M. Yamaguchi, H. Yamada, J. Chida, K. Shilata, H. Kido. Thermal instability of compound variants of carnitine palmitoyltransferase II and impaired mitochondrial fuel utilization in influenza-associated encephalopathy. Hum Mutat 29 (2008) pp. 718–727.

Zeviani et al., 1989 M. Zeviani, S. Servidei, C. Gellera, E. Bertini, S. DiMauro. An autosomal dominant disorder with multiple deletions of mitochondrial DNA starting at the D-loop region. Nature 339 (1989) pp. 309–311.

Zhang et al., 2012 M. Zhang, Y. Xu, T. Ouyang, J. Li, T. Wang, Z. Fan, TFB. Lin, Y. Xie. Somatic mutations in the *BRCA1* gene in Chinese women with sporadic breast cancer.Breast Cancer Res Treat 132 (2012) pp. 335-340

Zhang, 2013 J. Zhang. The role of BRCA1 in homologous recombination repair in response to replication stress: significance in tumorigenesis and cancer therapy. Cell &

Bioscience 3: 11 (2013)

Zhao et al., 2013 F. Zhao, J. Wu, A. Xue, Y. Su, X. Wang, X. Lu, Z. Zhou, J. Qu, X. Zhou. Exome sequencing reveals CCDC111 mutation associated with high myopia. Hum Genet 132 (2013) pp. 913–921.

Figure legends

Figure 1

Pedigree of the family (A); brain MRI of the proband (B); PCR–Southern blot analysis (C); and Sanger sequencing analysis (D).

In the family pedigree, the proband is indicated by an arrow (A). Black segments in symbols indicate the presence of disease symptoms. The upper left, lower left, upper right, and lower right black quarters indicate ptosis, hearing loss, mental retardation or cognitive dysfunction, and diabetes, respectively. Asterisks indicate stroke. A single dot indicates individuals who provided blood samples for this study. Brain MRI of the proband revealed general cerebral atrophy on T1- and T2-weighted and FLAIR images (B). T2-weighted and FLAIR images show symmetrical high-signal-intensity spots in the deep white matter, basal ganglia, thalamus, and frontal periventricular high-intensity regions. Both the spots and the periventricular regions correspond to the low-signal-intensity region on T1-weighted images. The PCR–Southern blot analysis was performed using total muscle DNA (M) and leukocyte genomic DNA (L) (C). Multiple deletions were observed in the muscle mtDNA of the proband (Lane 7). In contrast, no deletions were observed in the PCR–Southern blot analysis of leukocyte DNA from the control, the proband, II–2, II–3, III–10, or IV–1 (Lanes 1–6, respectively). The results of the Sanger sequencing analysis of the proband (D) show heterozygous c.265T>G in *PRIMPOL*, c.824G>A in *BRCA1*, 1813G>C, c.1055T>G, and c.1102G>A in *CPT2*, homozygous c.235delC in *GJB2*, 289_290insAA in *CARD8*, and c.329T>C and c.442G>C in *MEFV*.

Figure 1

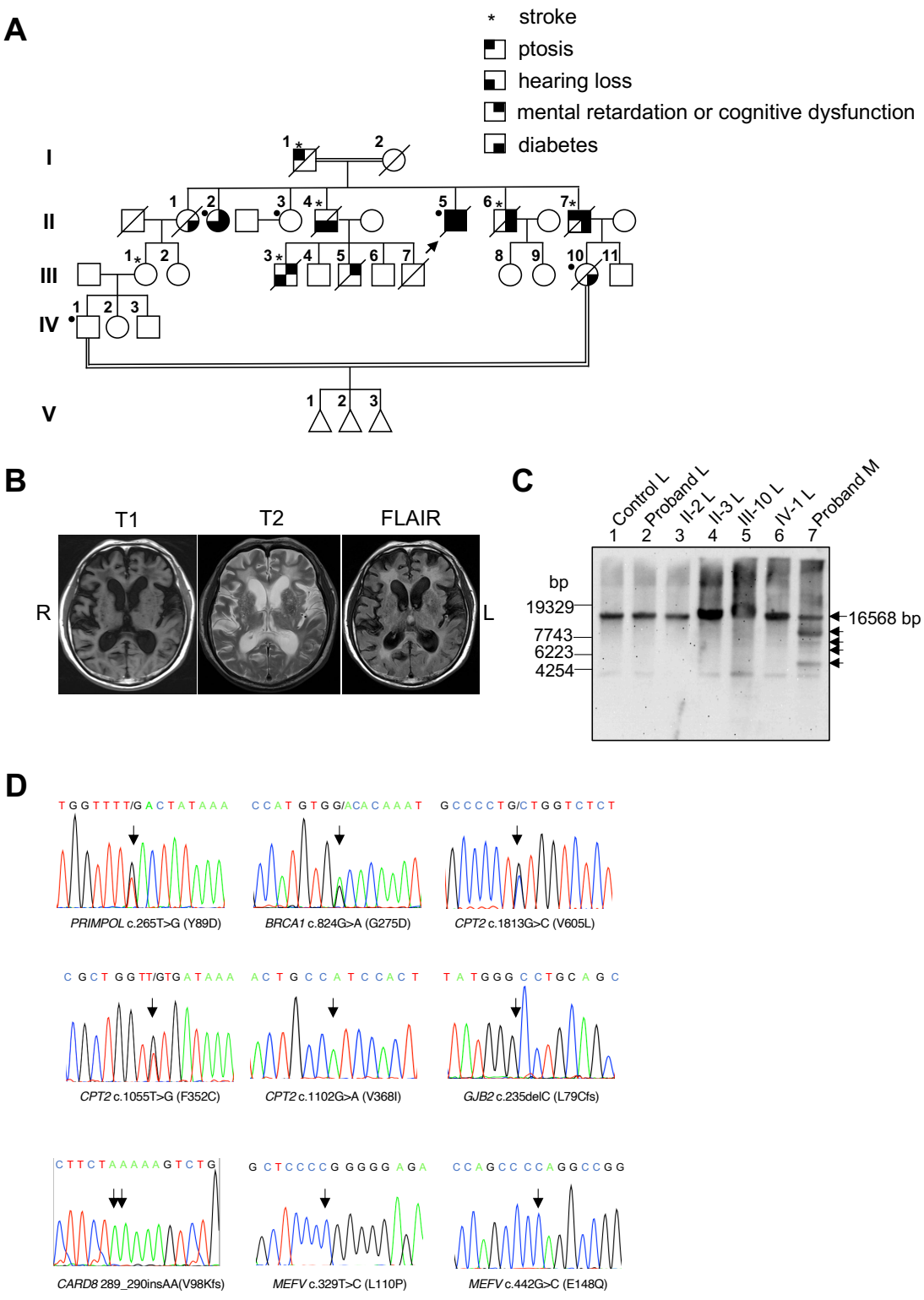
A
* stroke
ptosis
hearing loss
mental retardation or cognitive dysfunction
diabetes
I
II
III
IV
V
B
T1
T2
FLAIR
R
L
C
Control L
Proband L
II-2 L
II-3 L
III-10 L
IV-1 L
Proband M
1 2 3 4 5 6 7
bp
19329
7743
6223
4254
16568 bp
D
PRIMPOL c.265T>G (Y89D)
BRCA1 c.824G>A (G275D)
CPT2 c.1813G>C (V605L)
CPT2 c.1055T>G (F352C)
CPT2 c.1102G>A (V368I)
GJB2 c.235delC (L79Cfs)
CARD8 289_290insAA(V98Kfs)
MEFV c.329T>C (L110P)
MEFV c.442G>C (E148Q)

Table 1 Summary of filtering procedure used to narrow down candidates for phenotype-related variants

General information before filtering	
Total sequence length	6.3 Gb
Total number of variants	123712

Criteria for heterozygous variations	Number of remaining variants
Variants in genes associated with “mtDNA” or “replication” (GeneCard®)	91
Coverage > 10	80
Very rare variants (MAF $\leq$ 0.1%)	4
Cosegregate with the phenotypes of the proband and II-2	3

Criteria for homozygous variants	Number of remaining variants
Homozygous variants	4546
Coverage > 10	4280
Very rare variants (MAF $\leq$ 0.1%)	29
Not benign by PolyPhen-2	21
Cosegregate with the phenotype	1

Table 2 Cosegregation of variants in *GJB2, PRIMPOL*, *BRCA1*, *CPT2, CARD8* and *MEFV.*

	Mutations				Polymorphisms				
	GJB2	*PRIMPOL*	*BRCA1*	*CPT2*	*CPT2*		*CARD8*	*MEFV*	
Variant	235delC	265T>G	824G>A	3G>C	1055T>G	1102G>A	289_290insAA	329T>C	442G>C
					rs2229291	rs1799821	rs140826611	rs11466018	rs3743930
	L79Cfs	Y89D	G275D	V605L	F352C	V368I	V98Kfs	L110P	E148Q
MAF	-	0.0007	0.0010	0.0002	0.1778	0.6787	0.0525	0.0638	0.2129
Poly-Phen-2 score	-	0.975	0.997	0.885	-	-	-	-	-
The proband	delC/delC	T/G	G/A	G/C	T/G	A/A	insAA/insAA	C/C	C/C
II–2	delC/delC	T/G	G/A	G/C	G/G	A/A	insAA/insAA	T/T	G/G
II–3	C/C	T/T	G/G	G/G	T/G	A/A	normal/normal	C/C	C/C
III–10	C/C	T/T	G/G	G/G	T/T	A/A	insAA/normal	T/T	G/G
Ⅳ–1	C/C	T/T	G/G	G/G	T/G	A/A	normal/normal	T/T	G/G

MAF, minor allele frequency, calculated by the Japanese reference panel project of the Tohoku Medical Megabank (2KJPN). Alternative alleles include nucleotides, and amino acids are underlined.

Supplementary Table

Primers used for amplification and sequencing.

Primers sequences for nuclear genes	
RRM2B	
Exon1F: CTTGCCGAGACAGGGATAAT	Exon1R: GCGGCGAATAACATTTCCTA
Exon2F: GATTCAACCCAGGCAGACAG	Exon2R: TCTTCTACAACTGATCTTCTTCAATG
Exon3F: TTCTTTGCAGTGCTAACATCTTTC	Exon3R: AGACATCTTGTCTTTGGCTGAA
Exon4F: CCATAAGGTCTTTCTGACCTGTTT	Exon4R: TGCTCAGAAACTTCCATACTTGA
Exon5F: CTTTGCTGTTCATTCTTTTGTTTT	Exon5R: CCTTAGGCAAATCTGATCATACA
Exon6F: AAAAATTGAAACGATTTTATGTCTCC	Exon6R: GATGGAAAAGAAAAATAGATGAACA
Exon7F: ACCCCTCTTCCATTTTCCAG	Exon7R: GGCTGACCAGAATAAAATTGC
Exon 8F: TGCCACATTGAAAGAATTTATCC	Exon8R: TGTTCATACAAAACAAGTCTCTGTCA
Exon 9F: GGGGAATGATATGATCTTGTAGC	Exon9R: AGCAAACCCCCAGTCCTTTA
GJB2	
GJB2F: CTTTTCCAGAGCAAACCGCC	GJB2R: TGGAGAAGCCGTACATG
PRIMPOL	
PRIMPOL-F: TGAATGGCATAAACCTAGTGACT	PRIMPOL-R: CTCCCTTTGAGTACACGCAT
BRCA1	
BRCA1F: GGTGTGGTTTCTGCATAGGGA	BRCA1R: TTTTCTGTGCTGGGAGTCCG
CPT2	
Exon 4F: TTGTGAGCCCCTCGGAAATC	Exon4R: TCCTTAGCAGCTGTGATGCC
Exon 5F: TAGAGCCTTCCCCCACTCTC	Exon5R: GACCTCAAGTGATCCACCCG
CARD8	
CARD8F: GGTGCATTGGTTCCAGTCCT	CARD8R: CCTCCCAAAGTGCCGAGATT
MEFV	
MEFV-F: ATCTTGGGCCCTAAACGTGG	MEFV-R: AATTTCTGGATTTGCGGGCG